Kuroshio Large Meander in an Eddy Resolving Ocean Model

Niklas Schneider[1,2], Bo Qiu[2] and Hideharu Sasaki[3]

[1]International Pacific Research Center, [2]Department of Oceanography, University of Hawaii, Honolulu, Hawaii, [3]Earth Simulator Center, JAMSTEC, Yokohama, Japan

Introduction

Intrinsic oceanic variations of ocean jets are a source of decadal climate variance. Here we investigate a prominent example: the Kuroshio path to the south of Japan that shows pronounced decadal variations between a near-shore and Large Meander paths (Fig. 1).

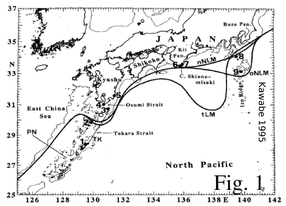

Fig. 1

We analyze an integration of the Ocean Model for the Earth Simulator, a MOM-3 type model with a horizontal resolution of 0.1° and 54 levels in the vertical, in a global domain from 75°S to 75°N. NCEP/NCAR reanalysis fluxes of momentum, heat and fresh water force the ocean in a 1950-2003 hindcast.

Kuroshio Variations

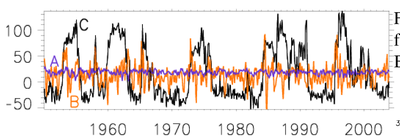

Fig. 2: Transports in Sv as function of time across sections A, B, C shown in Fig. 3.

Decadal scale fluctuations of the ocean transport in the Northwest Pacific (Fig. 2) indicate strong variations of the Kuroshio path. These are independent of upstream variations.

Sea level shows regionally confined, large variability (Fig. 3) south of Japan.

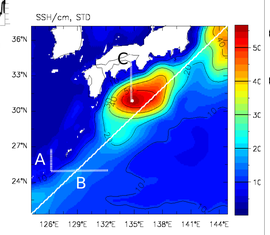

Fig. 3: Standard deviation of sea level. Dashed lines are sections used in Fig. 2.

Large Meander Index

The leading complex empirical orthogonal function (CEOF) of sea level anomalies south of Japan (130°E-141°E, 25°N-35°N) captures the Kuroshio path evolution. Its phase continuously decreases, and shows a decadal period. The magnitude is largest when the phase is close to π (Fig. 4).

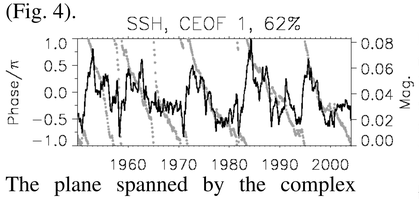

Fig. 4: Principal component of the leading CEOF of sea level in the Large Meander region south of Japan. The mode accounts for 62% of the variance.

The plane spanned by the complex principal component shows the clockwise, circular evolution (Fig. 5). We define the Large Meander index by the phase of 12 equal sectors measured from the geometric center of the shape, and form the composite of the Large Meander evolution.

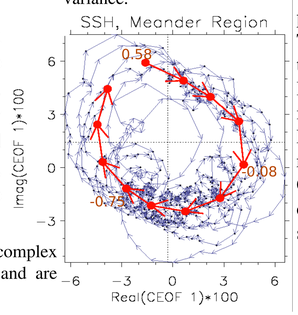

Fig. 5: Leading principal component in its complex space. Composite averages are shown in red and are referred to by their phase normalized by π.

Large Meander Evolution

The Large Meander index sorts the Kuroshio Paths defined by the 60 cm sea level height contour (Fig. 6). At phases of 0.42 and 0.25 the Kuroshio is in a straight path in agreement with observations (Fig.1). The meander develops at Izu Ridge, with an initial upstream trigger meander as in observations, and then propagates upstream. At phase -0.08 model and observed Large Meander are in agreement, but the simulated Meander continues to retrograde until the Kuroshio separates from the coast at Tokara Strait. Then, the system rapidly returns to a straight path.

The composite of sea level (Fig. 6) reflects this saw-tooth evolution, and shows the accompanying intensification of the recirculation gyres.

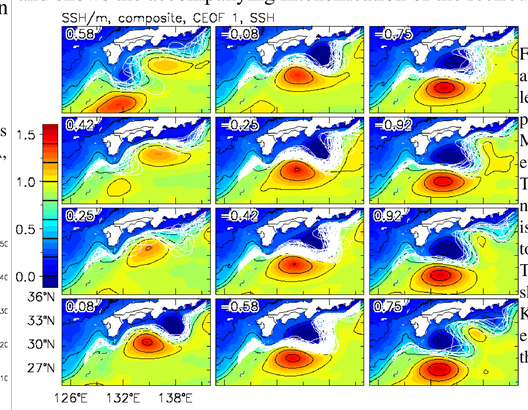

Fig. 6: Composite averages of sea level for each phase of the Large Meander evolution. The phase normalized by π is indicated in the top left corner. Thin white lines show the Kuroshio path for each member of the composite.

Potential Vorticity

The scatter of stream function and potential vorticity (PV) in the upper thermocline determines the degree of PV conservation (Fig. 7) and shows decreasing values of PV with stream function that reflects the average decrease of stratification with Ψ.

The scatter for Ψ values in the Kuroshio reflects the increase of PV at Tokara Strait and other capes, and the strong dependence of coastal vorticity generation on the Kuroshio path.

These coastal, high values of PV fill the cyclonic recirculation at low Ψ. Its PV decreases as the Kuroshio moves away from the coast as the Large Meander strengthens and retrogrades.

Concurrently at high Ψ, the anti-cyclonic recirculation spins up and slightly reduces its potential vorticity.

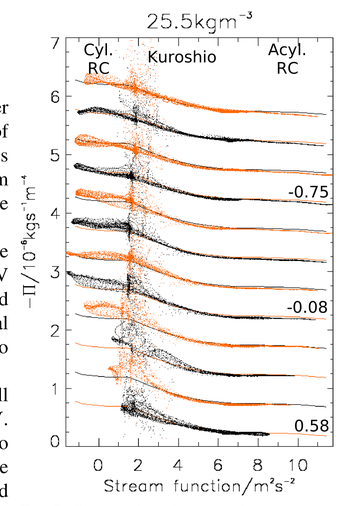

Fig. 7: Scatter plot of potential vorticity and stream function Ψ for each of the Large Meander state, as indicated by the phase on right. The line is the reference potential vorticity $f_0\partial\overline{\rho(\Psi)}/\partial z$. The stream function values for recirculation gyres and Kuroshio are indicated at top.

Path Kinematics

In the absence of dissipative processes, changes of relative vorticity due to a meandering Kuroshio path have to be balanced by other potential vorticity components. To explore these exchanges, PV is written in stream coordinates (Fig. 8) and normalized by $f_0\partial\overline{\rho(\Psi)}/\partial z$.

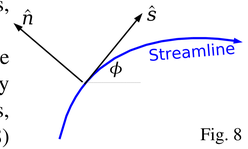

Fig. 8

$$\frac{PV}{\left(f_0\frac{\partial\bar{\rho}}{\partial z}\right)} - 1 = \frac{f'}{f_0} - \frac{\frac{\partial|v|}{\partial n}}{f_0} + \frac{|v|\frac{\partial\phi}{\partial s}}{f_0} + \frac{\frac{\partial\rho'}{\partial z}}{\frac{\partial\bar{\rho}}{\partial z}} + \frac{\zeta_h\nabla_h\rho}{f_0\frac{\partial\bar{\rho}}{\partial z}} + nonlinear$$

normalized PV — shear — curvature — thickness — tilt

The orbital vorticity is a small residual of the shear vorticity and vortex stretching (Fig. 9). The changes along the Kuroshio path indicate the impact of the anticyclonic recirculation. It affects shear vorticity by moving the center of the jet among stream lines, and by the divergence of the ageostrophic flow (gradient wind) that impacts vortex thickness. In addition, PV is not conserved and dissipative processes are important at the coast and in the jet.

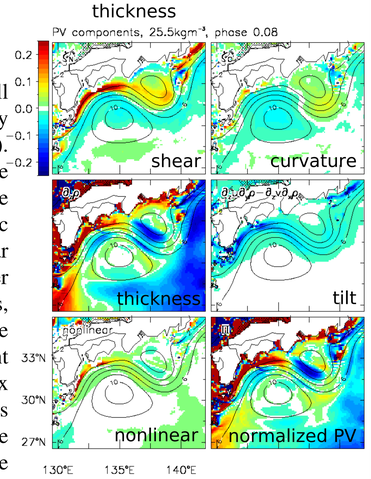

Fig. 9: Normalized components of potential vorticity on an isopycnal in the thermocline for phase 0.08 (color), and Montgomery stream function (contours).

Spin-up of Anti-Cyclonic Recirculation

The Large Meander system consists of a shallow cyclonic and a deep anticyclonic recirculation, and the Kuroshio jet. Of these, only the anticyclonic recirculation can support a multi-year time scale on par with the Large Meander.

As the Large Meander develops, the area and strength of the anticyclonic recirculation increase and suggest that the accumulation of low potential vorticity in this recirculation underlies the slow evolution of the Kuroshio path.

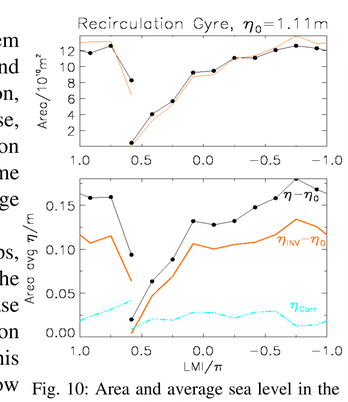

Fig. 10: Area and average sea level in the anticyclonic recirculation to the south of the Kuroshio (black lines), as a function of the Large Meander Index.

Forcing of the Anti-Cyclonic Recirculation

In the area south of Japan, the cumulative density function of PV shows an increasing occurrence of very low values during the build-up of the Large Meander. The appearance of this local PV minimum (Fig. 11) suggests surface diabatic forcing. However, this forcing is merely deepening further a dynamically preconditioned recirculation.

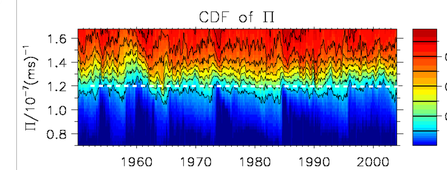

Fig. 11: Cumulative density function of PV in the region south of Japan, as a function of time in years. PV is estimated for the layer bounded by the surface and 26.0 isopycnal.

Low PV of the recirculation and in the tropics are not connected in the composite averages, but are linked by increased occurrences of low PV within the members of each composite (Fig. 12). The PV flux that feeds the build up of the anticyclonic recirculation is therefore due to fluctuations of the Kuroshio jet within each composite (Fig. 6) and due to eddies.

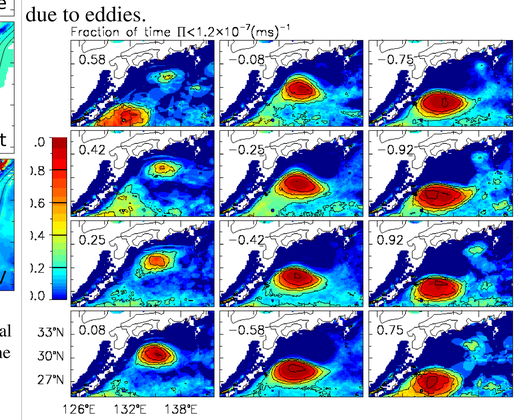

Fig. 12: Fraction of time PV is smaller than $1.2\times10^{-7}(ms)^{-1}$ for each Large Meander phase. Values range between zero (always larger than threshold) and one (always smaller than threshold).

Kuroshio Path Reset

Eventually, the Kuroshio system becomes unstable, sheds an eddy toward the southwest and returns to the straight path (Fig. 6). Spikes of deep ocean kinetic energy during these times suggest baroclinic instability.

Conclusion

- An unique ocean hindcast with an eddy resolving, global model produces vigorous variability of the Kuroshio path on decadal time scales.
- The evolution of the Kuroshio path passes through observed states, but culminates in an overly strong Large Meander with the Kuroshio separating from the coast at Tokara Strait.
- The Kuroshio path evolves in a saw-tooth fashion between straight path and Large Meander, and is governed by the slow spin-up of the recirculation gyre due to the advective accumulation of low potential vorticity.
- This behavior is likely sensitive to the parameterization of mixing: An increase of coastal mixing arrests the spin-up of the recirculation, and renders the system in steady state. Upstream conditions can then switch the system between possible steady states.